Entangling power of time-evolution operators in integrable and nonintegrable many-body systems

Rajarshi Pal and Arul Lakshminarayan
Department of Physics, Indian Institute of Technology Madras, Chennai 600036, India

(Received 7 June 2018; published 21 November 2018)

The entangling power and operator entanglement entropy are state-independent measures of entanglement. Their growth and saturation is examined in the time-evolution operator of quantum many-body systems that can range from the integrable to the fully chaotic. An analytically solvable integrable model of the kicked transverse-field Ising chain is shown to have ballistic growth of operator von Neumann entanglement entropy and exponentially fast saturation of the linear entropy with time. Surprisingly, a fully chaotic model with longitudinal fields turned on shares the same growth phase, and is consistent with a random matrix model that is also exactly solvable for the linear entropy entanglements. However, an examination of the entangling power shows that its largest value is significantly less than the nearly maximal value attained by the nonintegrable one. The importance of long-range spectral correlations, and not just the nearest-neighbor spacing, is pointed out in determining the growth of entanglement in nonintegrable systems. Finally, an interesting case that displays some features peculiar to both integrable and nonintegrable systems is briefly discussed.

DOI: 10.1103/PhysRevB.98.174304

I. INTRODUCTION

Effects of nonintegrability in quantum systems, dubbed quantum chaos or chaology [1–3], is now being vigorously studied in many-body systems with motivations ranging from thermalization and localization transitions to information scrambling [4–9]. While single-body quantum chaos engenders states behaving like those chosen from a uniform distribution over the Hilbert space [2], in many-body contexts it is fair to say that little is known about detailed statistical properties of stationary or time-evolving states. One important window into this is provided by various types of entanglements in the states [10–12]. For example, in bipartite systems a chaotic evolution rapidly entangles the two subsystems to nearly the maximum possible extent even when they are initially product states [13,14].

The most well-studied entanglement is that between two halves of many-body systems such as spin-chains, the block-entropy [15]. Natural questions of importance are how fast such an entanglement grows for initially unentangled states, the extent it reaches or saturates, and what distinguishes integrable and chaotic systems in these contexts [11,16–19]. In integrable critical systems described by a conformal field theory and the transverse Ising model, it was shown to grow linearly with time t before it saturates to a value dependent on the initial state [20]. Such a ballistic growth of entanglement was also seen, somewhat surprisingly, in a nonintegrable Ising model with longitudinal fields where energy transport itself is diffusive [21].

Compared with a nonintegrable case, the integrable one may entangle certain initial states faster and to a larger extent, while others lesser. Thus it is desirable and interesting to consider entanglement measures that are independent of the initial state. Two approaches present themselves, the first wherein the operator entanglement of propagators in time are studied. This was recently adopted in Ref. [22], where a many-body Floquet nonintegrable system and the Heisenberg model with disordered fields were considered (see also Ref. [23] for an earlier discussion based on conformal field theory). It was shown by simulations that the time-evolution operator entanglement entropy shows a linear, power-law, and logarithmic growth, respectively, for the Floquet system, the Heisenberg model in the weak disorder phase, and the many-body-localized phase [24,25].

The second approach is based on the notion that it is illuminating to look directly into the ability of time-evolution operators to create entangled states starting from *arbitrary* product states. As state entanglement is an important resource in information processing tasks, entangling abilities of unitary gates and entanglement of operators as a dynamical resource [26] have been considered. In particular, bipartite entangling power of an unitary operator has been defined as the average entanglement created when acting on a uniform distribution of product states [24,25]. This was shown in Ref. [25] to be related to operator entanglement entropy in a nontrivial way when defined via the linear entropy. This has been applied previously, for example, to quantum transport in light-harvesting complexes [27] and characterization of quantum chaos [28,29].

Using both approaches here, we study the entangling power and operator entanglement entropy of the unitary time-evolution operators $U(t)$ for simple spin chains in both integrable and nonintegrable regimes. Freed from the specificity of the initial state, we study the rate of growth of these quantities, their eventual saturation values if any, and compare them with a random matrix theory (RMT) model. We find analytically, ballistic growth of operator entanglement and evaluate entangling power in a particular case of the integrable transverse Ising model, reflecting the ballistic growth of state entanglement [20]. As in the case of states, it is found that the operator entanglement of certain integrable models can outstrip that of nonintegrable models, calling

into question the superior entangling capabilities of chaos [13,14,30,31]. However, we show that the entangling power in the same models is higher for the nonintegrable case, underlining the role of entangling power as opposed to operator entanglement.

The RMT model replaces the blocks between which the entanglement is found by random operators while retaining the interaction and is thus a hybrid one which is seen to be sometimes surprisingly good. While it can be expected to work for nonintegrable spin chains, the ballistic growth implied in some cases also leads to coincidence of the RMT with integrable models in the growth phase, partially resolving the ballistic growth seen in both integrable and nonintegrable cases.

RMT models serve as a good foil for many nonintegrable cases of the spin chains, as there is a correlation between the commonly used spectral property of the nearest-neighbor spacings (NNS) and how well the RMT model works. However, we also find that there are nonintegrable models with Wigner distribution of the NNS but yet do not follow the RMT model for entangling power just as well. This prompts the study of long-range spectral correlations such as number-variance, which shows differences amongst these nonintegrable cases. This demonstrates that long-range correlations that affect short-time behaviors are important in understanding the growth of entanglement in these systems than simply the NNS alone.

II. PRELIMINARIES

A. Measures, the ancilla picture, and Haar averages

Most measures of entanglement strengths of an operator U [26] acting in a bipartite space $\mathscr{H}_A \otimes \mathscr{H}_B$, $\dim(\mathscr{H}_{A,B}) = N$ are based on its Schmidt decomposition, $U = N \sum_{i=1}^{N^2} \sqrt{\lambda_i}\, A_i \otimes B_i$, with A_i and B_i being orthonormal operators on $\mathscr{H}_{A,B}$ satisfying, $\mathrm{Tr}(A_i^\dagger A_j) = \mathrm{Tr}(B_i^\dagger B_j) = \delta_{ij}$, $\lambda_i \geqslant 0$. If U is unitary, as will be the case in this work, then $\sum_i \lambda_i = 1$. We will consider operator entanglement entropies defined via both the linear and von Neumann entropies as

$$E_l(U) = 1 - \sum_{i=1}^{N^2} \lambda_i^2, \quad E_{vN}(U) = -\sum_{i=1}^{N^2} \lambda_i \log \lambda_i. \tag{1}$$

These vanish iff U is a tensor product of two operators.

Following Ref. [24], the entangling power of a unitary operator is defined as $\mathrm{ep}(U) = \overline{\mathscr{E}(|\psi\rangle = U|\psi_A\rangle|\psi_B\rangle)}^{|\psi_A\rangle,|\psi_B\rangle}$ with $\mathscr{E}$ being a suitable entanglement measure of *states* and the average is taken over all the product states $|\psi_A\rangle$, $|\psi_B\rangle$ distributed uniformly. In this paper, we consider $\mathscr{E}$ to be either the linear or von Neumann entropy of the reduced density matrix $\rho_A = \mathrm{Tr}_B(|\psi\rangle\langle\psi|)$, that is, $\mathscr{E}_L = 1 - \mathrm{Tr}(\rho_A^2)$ and $\mathscr{E}_{vN} = -\mathrm{Tr}(\rho_A \log \rho_A)$, respectively. The corresponding entangling powers are denoted by $\mathrm{ep}_l(U)$ and $\mathrm{ep}_{vN}(U)$.

While the entangling power has a natural interpretation as the average entanglement that is created by the action of U on arbitrary product states, it was shown in Ref. [24] that $\mathrm{ep}_l(U)$ is intimately connected to the operator linear entanglement entropy $E_l(\cdot)$ as

$$\mathrm{ep}_l(U) = \frac{N^2}{(N+1)^2}(E_l(U) + E_l(US) - E_l(S)), \tag{2}$$

where S is the swap operator $S|\psi_A\rangle|\psi_B\rangle = |\psi_B\rangle|\psi_A\rangle$. Additionally, we also find $\mathrm{ep}_{vN}(U)$ for which there is no such simple connection known to $E_{vN}(\cdot)$ and hence resort to finding it numerically.

To emphasize the qualitative difference between operator entanglement and entangling power of operators, we briefly recall the ancilla interpretation of the former [32], wherein we imagine that A and B are equipped additionally with N dimensional systems A' and B'. Let AA' and BB' be in the standard maximally entangled state $|\phi^+\rangle = \sum_{j=1}^N |jj\rangle/\sqrt{N}$, and consider the four-party state $|\Phi_U\rangle = (U_{AB} \otimes \mathbb{1}_{A'B'})|\phi^+\rangle_{AA'}|\phi^+\rangle_{BB'}$, where $U_{AB} \equiv U$. Then $E_{l,vN}(U)$ ($E_{l,vN}(US)$) are the linear and von Neumann entropies of the reduced state $\rho_{AA'} = \mathrm{Tr}_{BB'}(|\Phi_U\rangle\langle\Phi_U|)$ ($\rho_{AB'} = \mathrm{Tr}_{A'B}(|\Phi_U\rangle\langle\Phi_U|)$). These reduced states can also be related to reshuffling and partial transpose of U, allowing for their direct evaluation [33]. The central difference therefore is that operator entanglement can be viewed as the entanglement in one particular four-party state engendered by the action of a bipartite unitary operator, while the entangling power is the average entanglement in an ensemble of states resulting from its action on all two-party product states.

Averages over the Haar measure of unitary operators on $\mathscr{H}_A \otimes \mathscr{H}_B$, are important to compare with the saturation values for nonintegrable models. Thus we state known results [22,24,34]:

$$\overline{\mathrm{ep}_l} = (N-1)^2/(N^2+1), \ \overline{E_l} = (N^2-1)/(N^2+1),$$
$$\overline{E_{vN}} \approx 2\log N - 1/(2\ln(2)). \tag{3}$$

While $\overline{\mathrm{ep}_{vN}}$ is unknown, it is close to the Haar averaged value for pure states [35], namely $\log(N) - (1/(2\ln(2))$. These are simply referred to ahead as RMT averages.

B. The spin models

We consider the following Floquet Hamiltonian for a spin chain of L sites: $H(t) = H_0 + V \sum_{k=-\infty}^{+\infty} \delta(k - t/\tau)$, with

$$H_0 = \sum_{j=1}^{L-1} \sigma_j^z \sigma_{j+1}^z + \sum_{j=1}^{L} h_i^z \sigma_i^z, \quad \text{and}$$
$$V = \sum_{j=1}^{L} \left(h_j^x \sigma_j^x + h_j^y \sigma_j^y\right), \tag{4}$$

a kicked version of the Ising model with a magnetic field which has both transverse and longitudinal components. The model is integrable [30] for purely transverse ($h_i^z = 0$) or purely longitudinal ($h_i^x = h_i^y = 0$) fields and nonintegrable otherwise.

The state (in $\hbar = 1$ units) just after the $(n+1)$th kick is connected to the state just after the nth kick by the unitary Floquet operator: $|\psi(n+1)\rangle = |\psi(n) = U(\tau, h)|\psi(n)\rangle$, with

$$U(\tau, h) = e^{-iV\tau} e^{-iH_0\tau}. \tag{5}$$

The present work considers the bipartite entangling power and operator entanglement entropies of $U^n(\tau, h)$ between the first half and the rest of the spins, the dimension of the single-party Hilbert space thus being $N = 2^{L/2}$. As $\tau \to 0$, the kicked model goes over to a continuous time evolution and the discussions below therefore can be extended to time-independent Hamiltonians via the Suzuki-Trotter decomposition of the propagator.

We consider the following nonintegrable and integrable magnetic field configurations referred to as Set-NI: $(h_i^x = 0.9045, h_i^y = 0.3457, h_i^z = 0.8090)$ and Set-I: $(h_i^x = 1.0, h_i^y = 0, h_i^z = 0)$, respectively. The nonintegrable configuration is chosen mainly for comparison with literature [21,22] and not because of any fine-tuning. While we consider various values of τ, the case $\tau = \pi/4$, is special as we exactly solve for the operator entanglement entropy and entangling power for the integrable case. Also, for the chosen nonintegrable configuration at this value of τ, the Floquet operator seems "maximally random" going beyond that captured by NNS distribution discussed in Ref. [21].

C. A hybrid RMT model

The spin Floquet operator in Eq. (5) is of the form $U(\tau, h) = (U_A \otimes U_B)\, U_{AB}(\tau)$ where $U_{A,B}$ are local to blocks A and B consisting of spins $1, \cdots, L/2$ and $L/2+1, \cdots, L$, respectively, and $U_{AB}(\tau) = \exp\{-i\tau\sigma^z_{L/2}\sigma^z_{L/2+1}\}$ is the nonlocal interaction between the blocks. While the local operators, which contain all the information of the fields, do not contribute to the entangling power of U itself, they play a crucial role for the powers U^n we are interested in [33]. The RMT model $U_{\rm RMT}(\tau)$ is a hybrid one wherein we replace $U_{A,B}$ by local random unitary matrices and retain the interaction as-is. As $U_{A,B}$ are merely $L/2$ length chains of the original kind, this can be expected to be a reasonable model if $U(\tau, h)$ is sufficiently nonintegrable and possesses random matrix properties.

Such models have been used to study spectral and entanglement transitions in coupled chaotic bipartite systems [36,37]. Random circuit models [38,39] have been used for many-body systems and to study the growth of initially local operator [40], and will be useful in the context of entangling power as well. However, as we are considering bipartite entanglements and there are analytical results available if the local block operators are fully random we adopt this caricature.

III. OPERATOR ENTANGLEMENT ENTROPY VS ENTANGLING POWER

A. RMT model predictions

While quantities such as $\langle E_l[U^n_{\rm RMT}(\tau)]\rangle_{\rm loc}$, where $\langle\cdot\rangle_{\rm loc}$ denote averages over the local random operators are of interest, they are harder to compute than one wherein the local operators are independent random matrices U_{Aj}, U_{Bj} at different times j. In this case, analytical results are possible for the case of operator linear entanglement entropy and corresponding entangling power [33], for example, results therein imply an exponential growth of entangling power:

$$\begin{aligned}\left\langle \mathrm{ep}_l\left(U^{(n)}_{\rm RMT}(\tau)\right)\right\rangle_{\rm loc} &= \overline{\mathrm{ep}_l}\left[1-\left(1-\frac{\mathrm{ep}_l(U_{AB}(\tau))}{\overline{\mathrm{ep}_l}}\right)^n\right]\\ &= \overline{\mathrm{ep}_l}\left[1-\left(1-\frac{C_N}{2}\sin^2(2\tau)\right)^n\right],\end{aligned} \tag{6}$$

with $C_N = N^2(N^2+1)/(N^2-1)^2 \approx 1 + 3/N^2$ and using Eqs. (3) $\overline{\mathrm{ep}_l} \approx 1 - 2/N$. The braces in $U^{(n)}$ indicates that the local operators vary with time and averages are with respect to the circular unitary ensemble (CUE) sampling the space of unitaries in $\mathscr{H}_{A,B}$ uniformly.

We have verified that the averages do not change if we choose the same CUEs for both U_{Aj} and U_{Bj} for a particular time j or even choose a single CUE for both for all j, as is the case with the spin model. Thus we can expect these to provide estimates for $U^n(\tau, h)$. There are also similar expressions for averages of $E_l(U^n)$, $E_l(U^n S)$ [33], which results in

$$\left\langle E_l\left(U^{(n)}_{\rm RMT}(\tau)\right)\right\rangle_{\rm loc} \approx 1 - \left(1 - \tfrac{1}{2}\sin^2(2\tau)\right)^n, \tag{7}$$

where the approximation neglects terms of order $1/N^2$. Apart from the factor $\overline{\mathrm{ep}_l}$, this is just the entangling power and hence the operator entanglement and entangling power for the RMT model are essentially the same. We note that this already singles out $\tau = \pi/4$ as a case of maximal growth of entangling power, when $\mathrm{ep}_l(U^n)$ and $E_l(U^n)$ can be expected to grow as $1 - 2^{-n}$ when the magnetic field configurations lead to nonintegrable chains. For measures based on the von Neumann entropy, we resort to numerically computing the average over many CUE realizations. It may be pointed out that the value of $\tau = 0.8$ used in Ref. [22] is in fact very close to $\pi/4$ and we expect and find qualitatively identical results.

B. Operator entanglement entropy

The operator entanglement entropies $E_l(U^n)$ and $E_{vN}(U^n)$ as a function of time n, the number of kicks, is shown in Fig. 1 for $\tau = \pi/4$. These are exactly solvable for the integrable model (Set-I) as the λ_i in the Schmidt decomposition of $U^n(\pi/4, 1, 0, 0,)$ are all equal to $1/2^n$ for $0 \leqslant n \leqslant L$. This is most transparent on using Majorana fermions, however; in the next subsection we provide a proof based on Pauli spin operators. During this time we get simply

$$E_l(U^n) = 1 - 2^{-n}, \quad E_{vN}(U^n) = n. \tag{8}$$

Remarkably the $E_l(U^n)$ for the integrable chain coincides exactly with that for the RMT model, and thus both increase at the maximum rate. While we do not have a formula for the E_{vN} of the RMT model, the numerical simulation in Fig. 1 shows that it shares the linear growth for a long time till just before $n = L$ it turns and saturates to the value $\approx 2\log N - 1/(2\ln 2) \approx 9.28$, as $L = 10$. Quite surprisingly, the nonintegrable model increases just as much as the integrable model does, getting nearly maximally entangled at $n = L$, before disentangling and relaxing to the RMT average.

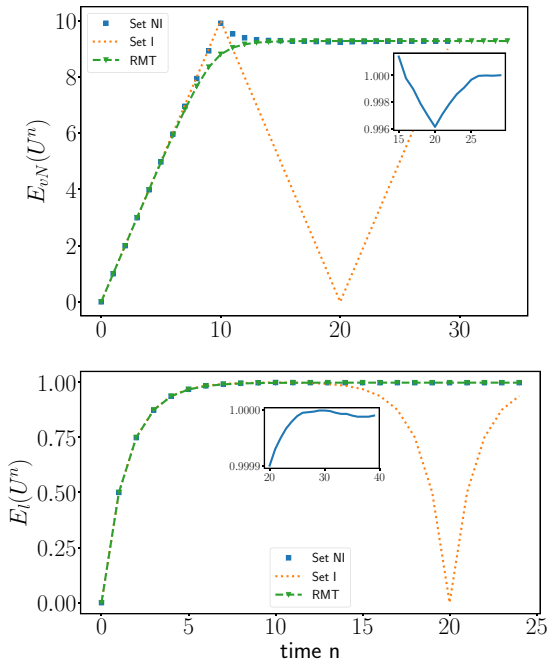

FIG. 1. Operator von Neumann (top) and linear (bottom) entanglement entropies, $E_{vN,l}(U^n(\tau,h))$ for nonintegrable (Set NI) and integrable cases (Set I), with $\tau=\pi/4$ and $L=10$ spins. Also shown are the corresponding RMT model results. Inset shows the ratio of the entropies for the nonintegrable model with the corresponding RMT averages from Eqs. (3).

C. Analytical treatment of the operator entanglement entropy for the integrable case

We consider the integrable kicked Ising model, with the parameters in Set-I ($h_i^x=1.0, h_i^y=0.0, h_i^z=0$) and time between kicks $\tau=\pi/4$. The time evolution or Floquet operator, we recall, is thus given by

$$U=\exp\left(-i\frac{\pi}{4}\sum_{j=1}^{L}\sigma_j^z\sigma_{j+1}^z\right)\exp\left(-i\frac{\pi}{4}\sum_{j=1}^{L}\sigma_j^x\right). \quad (9)$$

Introduce the following notation for spin operators of different partitions, for $j\leqslant M=L/2$,

$$\vec{A}_j\equiv\vec{\sigma}_{M+1-j}, \quad \text{and } \vec{B}_j\equiv\vec{\sigma}_{M+j}. \quad (10)$$

Thus A_1 and B_1 represent Pauli matrices for spins at locations M and $M+1$, respectively, see Fig. 2.

Local operators are those that belong exclusively to the space of A or B spins. It was shown in Ref. [41] that the *nonlocal* part of U^n is $(U^n)_{nl}=\prod_{i=1}^{n}V_i$, where the mutually commuting operators V_i are given by

$$V_i=\frac{1}{\sqrt{2}}\left(I-iA_i^yB_i^y\prod_{j=1}^{i-1}A_j^xB_j^x\right), \quad 1\leqslant i\leqslant L/2. \quad (11)$$

Beyond $i=L/2$ we have

$$V_{\frac{L}{2}+k}=\frac{1}{\sqrt{2}}\left(I-iA^z_{\frac{L}{2}-k+1}B^z_{\frac{L}{2}-k+1}\prod_{j=1}^{\frac{L}{2}-k}A_j^xB_j^x\right), \quad 1\leqslant k\leqslant L/2, \quad (12)$$

and $V_{L+k}=V_k$. It is also easy to see that V_j^2 is a local operator as far as the AB partition is concerned as

$$V_j^2=-iA_j^y\prod_{k=1}^{j-1}A_k^x\otimes B_j^y\prod_{k=1}^{j-1}B_k^x. \quad (13)$$

Note that V_1 and V_L involve only the A_1^y, B_1^y and A_1^z, B_1^z operators, respectively. The V_i contain precisely strings of operators that appear in the Jordan-Wigner transform of spins to Majorana fermions. Thus, although we can interpret the results elegantly in terms of entanglement between Majorana fermions of two species (those in A and B), we proceed with the spin language as it provides the Schmidt decompositions of operators written with spin variables. All the measures used in this work, $E_{l,vN}(U)$, $E_{l,vN}(US)$, $\mathrm{ep}_{l,vN}(U)$ are local operator invariants [33]; that is, they are the same as for $(U_A\otimes U_B)\,U\,(U'_A\otimes U'_B)$. They can hence be obtained by just considering the nonlocal part of $U^n\equiv(U^n)_{nl}$.

In this subsection, we find how the linear and von Neumann operator entanglement entropies grow with the number of kicks n. We do this by showing that as we multiply the operators V_i [Eq. (11)], in each step we get an operator Schmidt decomposition with equal Schmidt coefficients, with the Schmidt rank simply doubling at each step, till $n\leqslant L/2$. Thus, $(U^n)_{nl}$ is an operator with Schmidt rank 2^n, with equal Schmidt coefficients.

For, $i>L/2$ the structure of V_i changes, as in Eq. (12). Suppose we are interested in $n=L/2+m$, the strategy is to define m operators, $V'_{m+1-k}=V_{\frac{L}{2}+k}V_{\frac{L}{2}-k+1}$, $1\leqslant k\leqslant m$. We already know that, $\prod_{i=1}^{L/2-m}V_i$ is a maximally entangled operator with Schmidt rank $2^{(L/2-m)}$. We will then show, taking advantage of the commutativity of V_j, that multiplying with a V' quadrupules the Schmidt rank so that $(U^{\frac{L}{2}+m})_{nl}$ is an operator with Schmidt rank $2^{L/2-m}2^{2m}=2^n$. This immediately leads to the desired result.

Theorem 1. $E_l(U^n)=1-2^{-n}$, $E_{vN}(U^n)=n$, $E_{l,vN}(U^{2L-n})=E_{l,vN}(U^n)$, $1\leqslant n\leqslant L$.

Proof. First, assume that $n\leqslant L/2$. To begin with, notice by direct computation that

$$V_1=\frac{1}{\sqrt{2}}\left(I_1\otimes I_1-iA_1^y\otimes B_1^y\right),$$
$$V_2V_1=\tfrac{1}{2}\left(I_{12}\otimes I_{12}-iA_1^y\otimes B_1^y-iA_1^xA_2^y\otimes B_1^xB_2^y+A_1^zA_2^y\otimes B_1^zB_2^y\right),$$

are already in the Schmidt decomposed form except for the phases that can be absorbed into the operators. They

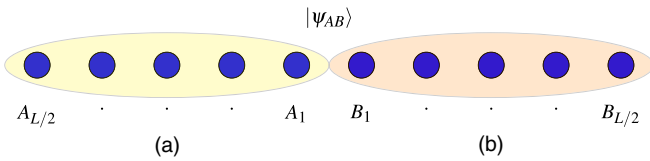

FIG. 2. Schematic of the labeling scheme used for the two partitions A and B.

are maximally entangled with entropies 1 and 2, respectively, as the Schmidt coefficients are $(1/\sqrt{2}, 1/\sqrt{2})$ and $(1/2, 1/2, 1/2, 1/2)$. To proceed by induction, assume that

$$\prod_{i=1}^{n-1} V_i = \frac{1}{2^{(n-1)/2}} \sum_{j=1}^{2^{(n-1)}} \mathscr{A}_j^{(n-1)} \otimes \mathscr{B}_j^{(n-1)}, \tag{14}$$

with $\mathrm{Tr}(\mathscr{A}_i^{(n-1)\dagger} \mathscr{A}_j^{(n-1)}) = \mathrm{Tr}(\mathscr{B}_i^{(n-1)\dagger} \mathscr{B}_j^{(n-1)}) = 2^{(n-1)}\delta_{ij}$.

Now,

$$V_n = \frac{1}{\sqrt{2}}\left(I - i A_n^y A_{n-1} \otimes B_n^y B_{n-1}\right), \tag{15}$$

with $A_{n-1} = \prod_{k=1}^{n-1} A_k^x$, $B_{n-1} = \prod_{k=1}^{n-1} B_k^x$. Thus,

$$V_n \prod_{i=1}^{n-1} V_i = \frac{1}{2^{n/2}} \sum_{j=1}^{2^{n-1}} \left(\mathscr{A}_j^{(n-1)} \otimes \mathscr{B}_j^{(n-1)} - i\left(A_n^y A_{n-1} \mathscr{A}_j^{(n-1)}\right) \otimes \left(B_n^y B_{n-1} \mathscr{B}_j^{(n-1)}\right)\right).$$

This is again Schmdit decomposed but for phases, as $A_n^y A_{n-1} \mathscr{A}_j^{(n-1)}$ is orthogonal to $A_n^y A_{n-1} \mathscr{A}_k^{(n-1)}$, for all $j \neq k$ (as $A_n^y A_{n-1}$ is unitary) and also $A_n^y A_{n-1} \mathscr{A}_j^{(n-1)}$ is orthogonal to $\mathscr{A}_k^{(n-1)}$, for $j \neq k$ as there is one extra spin from site n in the former. Identical considerations hold for B operators. Hence, with suitable redefinitions, we again have an orthogonal decomposition,

$$\prod_{i=1}^{n} V_i = \frac{1}{2^{n/2}} \sum_{j=1}^{2^n} \mathscr{A}_j^{(n)} \otimes \mathscr{B}_j^{(n)}. \tag{16}$$

With the normalization of the $\mathscr{A}^{(n)}$ operators as $\mathrm{Tr}(\mathscr{A}^{(n)\dagger} \mathscr{A}^{(n)}) = 2^n$, it follows that the 2^n Schmidt coefficients λ_j are all 2^{-n}. Thus the result follows.

For $n \geqslant L/2$, by virtue of Eq. (11),

$$V_{\frac{L}{2}-k+1} = \frac{1}{\sqrt{2}}\left(I - i A^y_{\frac{L}{2}-k+1} B^y_{\frac{L}{2}-k+1} \prod_{j=1}^{\frac{L}{2}-k} A_j^x B_j^x\right), \quad 1 \leqslant k \leqslant L/2. \tag{17}$$

Suppose we are interested in $E(U^{\frac{L}{2}+m})$, $(1 \leqslant m \leqslant L/2)$. Define m paired-up operators as follows:

$$\begin{aligned} V'_{m+1-k} &= V_{\frac{L}{2}-k+1} V_{\frac{L}{2}+k} \\ &= \tfrac{1}{2}\big(I - i A^z_{\frac{L}{2}-k+1} A_{L/2-k} B^z_{\frac{L}{2}-k+1} \\ &\quad \times B_{L/2-k} - i A^y_{\frac{L}{2}-k+1} A_{L/2-k} B^y_{\frac{L}{2}-k+1} \\ &\quad \times B_{L/2-k} + A^x_{\frac{L}{2}-k+1} B^x_{\frac{L}{2}-k+1}\big), \end{aligned} \tag{18}$$

with $1 \leqslant k \leqslant m$ and $A_{L/2-k} = \prod_{j=1}^{\frac{L}{2}-k} A_j^x$ and $B_{L/2-k}$ is similarly defined. Hence we have

$$E_{l,vN}(U^{\frac{L}{2}+m}) = E_{l,vN}\left(\prod_{j=1}^{\frac{L}{2}-m} V_j \prod_{l=1}^{m} V'_l\right). \tag{19}$$

From the first part of the proof, it is clear that $\prod_{j=1}^{\frac{L}{2}-m} V_j$ will have a Schmidt decomposition $\frac{1}{2^{\frac{n}{2}}} \sum_{j=1}^{2^n} \mathscr{A}_j^{(n)} \otimes \mathscr{B}_j^{(n)}$ of rank 2^n with $n = \frac{L}{2} - m$. Multiplying these with V'_j operators increases the Schmidt rank fourfold each time, each contains four orthogonal terms with a new spin operator at each step. Thus this follows on similar lines as for U^n with $n < L/2$, and we get that the Schmidt rank of $U^{L/2+m}$ is $2^{L/2-m} \times 4^m = 2^{L/2+m}$. Hence we have till $n = L$, $E_l(U^n) = 1 - 2^{-n}$, $E_{vN}(U^n) = n$.

Beyond $n = L$, the operator gets "disentangled" in a symmetric manner; that is, $E_{l,vN}(U^{2L-n}) = E_{l,vN}(U^n)$. This follows as U^{2L} is local across the $A|B$ partition, as its nonlocal part is

$$V_1^2 \cdots V_L^2, \tag{20}$$

and each V_j^2 are local. Thus $E(U^{2L-m}) = E(U^{-m}) = E(U^m)$, the last equality following from the fact that the Schmidt decomposition of an operator and its adjoint only differ in the Schmidt operators being self-adjoints of each other. Note that $E_{l,vN}(U^{2L}) = 0$ and the operator gets fully disentangled.

D. Entangling power

While these results may indicate superior entangling capabilities of the integrable model, except for its complete eventual disentanglement at $n = 2L$, it must be borne in mind that the operator entanglement is the result of acting on a particular pair of maximally entangled states involving ancillas. The entangling power, on the other hand, is the effect on a democratic choice of product states. Figure 3 shows the variation of $\mathrm{ep}_{l,vN}(U^n(\tau, h))$ for $\tau = \pi/4$. It is interesting that in contrast to the operator entanglement that continues to increase till L kicks for both the integrable and nonintegrable models, entangling power reaches a maximum at $n = L/2$ for the integrable model and starts decreasing, reaching a local minimum after L kicks. On the other hand, the nonintegrable model continues to increase during this time and saturates to the RMT value, the contrast being clearer in the von Neumann entropy.

The integrable model at $\tau = \pi/4$ can be exactly solved again for the linear entropy entangling power, and the result is given by the next theorem.

Theorem 2. The linear entropy entangling power for the integrable model is $\mathrm{ep}_l(U^n) = \frac{1+2^L-2^{L-n}-2^{n-1}}{(1+2^{L/2})^2}$, $1 \leqslant n \leqslant L$, with $\mathrm{ep}_l(U^0) = 0$.

Proof. Our starting point is the relation [25]

$$\mathrm{ep}_l(U) = \frac{N^2}{(N+1)^2}(E_l(U) + E_l(US) - E_l(S)). \tag{21}$$

As we already know, $E_l(U^n)$ from Theorem 1 we need $E_l(U^n S)$. This is obtained in Lemma 4 in Appendix B. The proof follows after elementary manipulations, on using Theorem 1 and Lemma 4 together with Eq. (21) and $E_l(S) = 1 - 1/2^L$.

Beyond this time, the entangling power is symmetric, that is, $\mathrm{ep}_l(U^{L+n}) = \mathrm{ep}_l(U^{L+n})$ and becomes zero at $n = 2L$ as U^{2L} is local across the bipartition. The maximum entangling power occurs at $n = L/2$ when it is for large $L \approx 1 - (7/2)2^{-L/2}$, while the nonintegrable model reaches the RMT average $\overline{\mathrm{ep}_l} \approx 1 - (2)\,2^{-L/2}$. Also, it is clear from

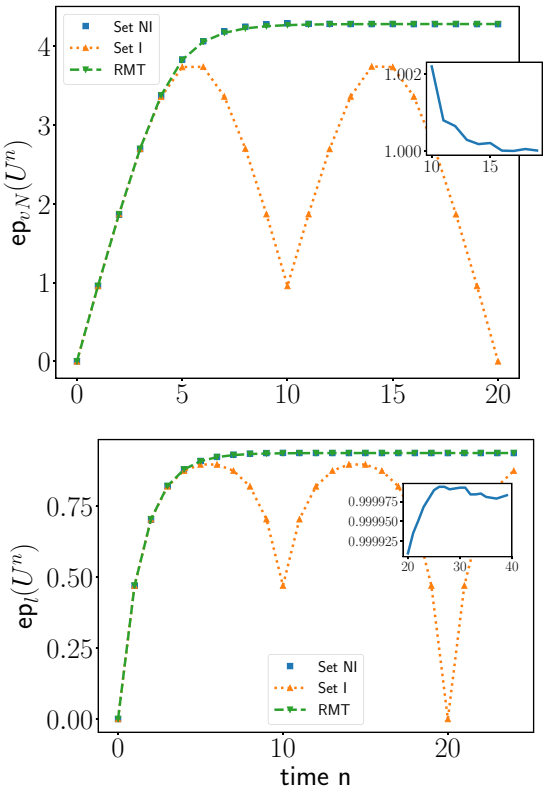

FIG. 3. The von Neumann (top) and linear (bottom) entangling powers, $\mathrm{ep}_{vN,l}(U^n(\tau,h))$ for the nonintegrable (Set-NI) and the integrable cases (Set-I), with $\tau=\pi/4$ and $L=10$ spins. Also shown are the corresponding RMT model results. Inset shows the ratio of the entangling powers for the nonintegrable model with the corresponding RMT averages in Eqs. (3).

Fig. 3 that the RMT model prediction for the entangling power based on the linear entropy in Eq. (6) works very well for the nonintegrable case at this value of τ. The RMT model works also for the von Neumman entangling power found numerically and the saturation is very close to that of random states: $\log(N)-1/(2\ln(2))\approx 4.28$ for $L=10$ spins.

Thus, in terms of ability to create entanglement on an average, the nonintegrable model in Set-NI can eventually swamp the integrable one in Set-I, even though their operator entanglement entropies grow at the same rate. An insight into this difference is provided by the behavior of $E_l(U^nS)$, which decreases considerably for the integrable model compensating for the increasing $E_l(U^n)$. In contrast, $E_l(U^nS)$ is nearly a constant for the nonintegrable model (see Fig. 4).

Using the ancilla interpretation of the operator entanglements, this is reflective of the fact that entanglement is shared in a more multipartite manner in the almost random states created by the nonintegrable evolution. The integrable evolution, on the other hand, in the ancilla picture leads to a state which has maximal entanglement across the $AA'|BB'$ cut, but little entanglement across the $AB'|A'B$ cut. These features are qualitatively seen to hold for the von Neumann entropy as well, even though we do not have a similar relation between von Neumann entangling power and operator von Neumann entropy.

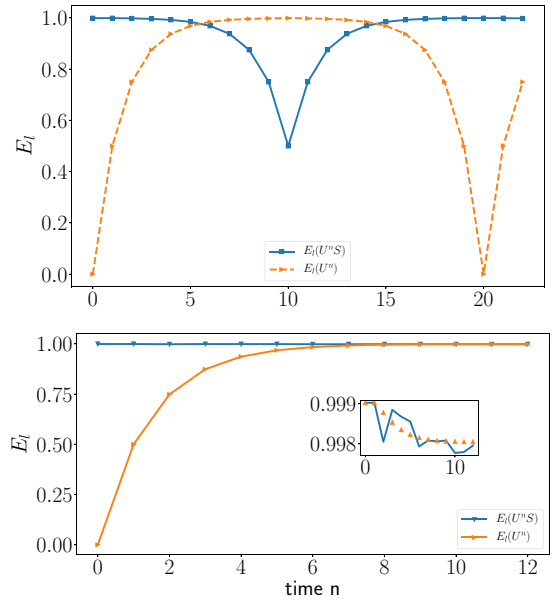

FIG. 4. Linear entropy operator entanglements $E_l(U^n(\tau,h))$ and $E_l(U^n(\tau,h)S)$ for integrable (Set-I, top) and nonintegrable cases (Set-NI, bottom), with $\tau=\pi/4$ and $L=10$ spins. Inset shows details of $E_l(U^n(\tau,h)S)$ for the nonintegrable case and also the RMT model prediction (triangles).

E. $\tau\neq\pi/4$: Correlations with the NNS distribution and number variance

For values of τ different from $\pi/4$, a varied scenario develops when comparing the integrable and the nonintegrable. The entangling power for $\tau=\pi/8$ is shown in Fig. 5. While the integrable may outstrip the nonintegrable in rate of entangling power, the nonintegrable eventually develops a larger value. Unlike in the case of $\tau=\pi/4$, in the integrable case this does not vanish and shows fairly small oscillations about what may be an equilibrium. Also, the RMT model predicts a larger power in the growth phase and is not as good as at $\tau=\pi/4$. It also appears that the saturation value of the entangling power and operator entanglement (not shown) is slightly smaller than

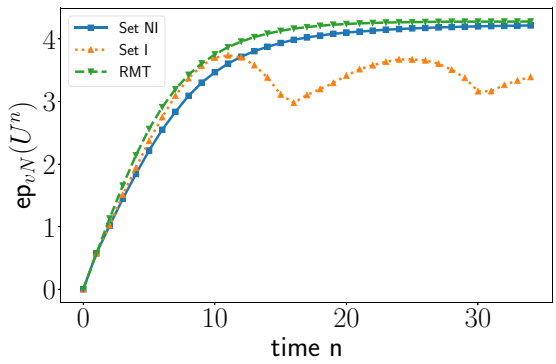

FIG. 5. The von Neumann entropy entangling power, $\mathrm{ep}_{vN}(U^n(\tau,h))$ for the nonintegrable Set-NI, integrable Set-I, with $\tau=\pi/8$ and $L=10$ spins. Also shown are the corresponding RMT model results.

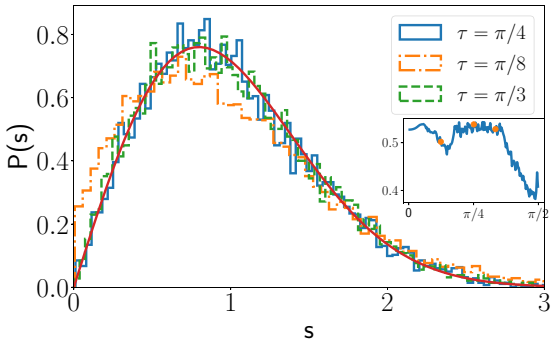

FIG. 6. Distribution of spacing for the nonintegrable Set-NI, with $\tau = \pi/3, \pi/4, \pi/8$ for $L = 14$. Inset shows the mean of the ratio of nearest-neighbor spacing distribution (NSS) of the operator U vs time between kicks τ. Dots in the inset correspond to $\tau = \pi/3$, $\pi/4$ and $\pi/8$.

the RMT value. These may be attributed to the fact that at $\tau = \pi/8$ the model is not quite as "chaotic" as at $\tau = \pi/4$.

This is borne out from the NNS distribution and ratio of spacings (using desymmetrized spectrum of even parity states) as illustrated in Fig. 6. While the nonintegrable cases with $\tau = \pi/4$ and $\pi/3$ fit the Wigner distribution

$$p_W(s) = \frac{\pi}{2}\, s\, \exp\left(-\frac{\pi}{4}s^2\right),$$

valid for systems with a time-reversal or in general an antiunitary symmetry, the case of $\tau = \pi/8$ shows significant deviations. Although the presence of the σ_y terms in the Hamiltonian may suggest time-reversal violation [22], it actually has a false-time-reversal violation and follows the statistics of the orthogonal ensemble COE. See Appendix A for details. The average of the ratio of spacings [42] shown in the inset is also close to the RMT value of 0.53 for $\tau = \pi/4$ and $\pi/3$, but is $\approx$0.49 for the case of $\tau = \pi/8$.

However, a puzzle arises in the case of $\pi/3$, which seems as RMT-like as the operator at $\pi/4$ in terms of NNS statistics. The behavior of the entangling power is shown in Fig. 7, and while the saturation value is that of the RMT model, in its growth phase it deviates significantly. Short-time properties are determined by long-range energy correlations [43] rather

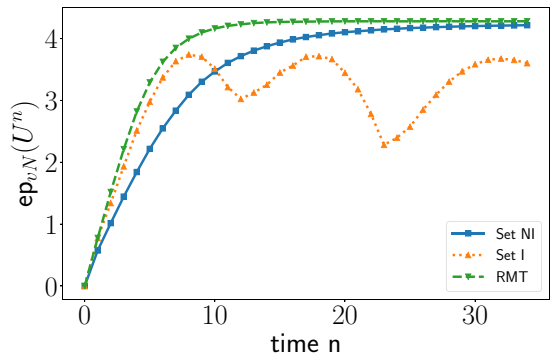

FIG. 7. The von Neumann entropy entangling power, $\mathrm{ep}_{vN}(U^n(\tau, h))$ for the nonintegrable Set-NI, integrable Set-I, with $\tau = \pi/3$ and $L = 10$ spins. Also shown are the corresponding RMT model results.

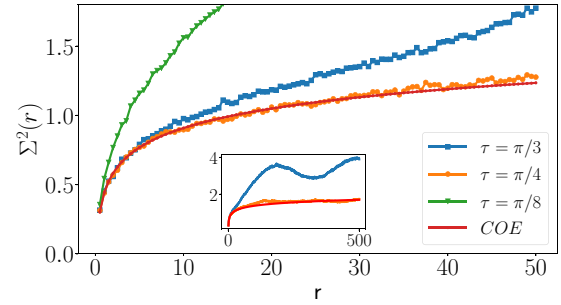

FIG. 8. Number variance for $\tau = \pi/3, \tau = \pi/4$, and $\tau = \pi/8$. Inset shows the same for $\tau = \pi/3, \pi/4$ in a longer range.

than the short-ranged NNS. For example, the number-variance [44] is one such quantity and is defined as $\Sigma^2(r) = \langle (n(r) - r)^2 \rangle_\Delta$, with $n(r)$ denoting the number of energy levels in an energy window of width r in an unfolded spectrum and $\langle \cdot \rangle_\Delta$ denoting average over length r windows. Figure 8 shows this quantity as a function of r for $\tau = \pi/8$, $\pi/4$ and $\pi/3$.

The number variance for the integrable case corresponds to the that of Poissonian statistics and is simply $\Sigma^2(r)_{\mathrm{Poiss}} = r$, while the COE number variance is given by

$$\Sigma^2(r)_{\mathrm{COE}} = 2\left[\frac{1}{\pi^2}(\ln(2\pi r) + \gamma + 1 - \cos 2\pi r - \mathrm{Ci}(2\pi r)) + r\left(1 - \frac{2}{\pi}\mathrm{Si}(2\pi r)\right)\right] + \left(\frac{\mathrm{Si}(\pi r)}{\pi}\right)^2 - \frac{\mathrm{Si}(\pi r)}{\pi}.$$

The number variances are shown in Fig. 8. While the case of $\tau = \pi/8$ deviates considerably from the RMT curve marked COE and is consistent with deviations found in the NNS. The case when $\tau = \pi/3$ agrees for about ten mean spacings and deviates thereafter, while $U(\pi/4)$ follows the RMT number variance over a much longer scale, with the inset showing agreement even at 500 level spacings. Thus, $\tau = \pi/3$ case is still intermediate to the Poisson or integrable limit and this is reflected in the short-time entangling power growth. Thus the study of long-range statistics in many-body systems may be crucial to distinguish those that are not fully chaotic. Unlike systems with a classical limit, these many-body systems are yet to be classified in terms of the extent of the chaos present.

F. A curious case

Finally, we display, very briefly, a case that has features of both the integrable and nonintegrable models, when for all i: $h_x^i = 1.0$, $h_y^i = 0$, $h_z^i = 1$ and $\tau = \pi/4$. Figure 9, top panel, shows the variation of operator entanglement entropy with the number of kicks in this model. This has exact time-periodicity such as seen in Fig. 1 for the integrable case. The system finally disentangles fully. The times at which this happens appears to be a nontrivial function of the number of spins L.

However, the entangling power, even if periodic, reaches as high a value as that of the nonintegrable case as shown in the bottom panel of Fig. 9. The entangling power also has minima at the same times as the operator entanglement; however, these are shallower. Being an interacting model, in

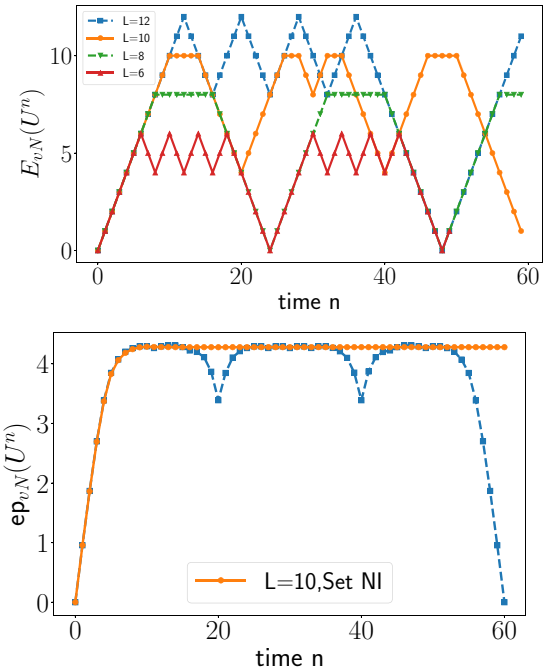

FIG. 9. Operator von Neumann entropy (top) $E_{vN}(U^n(\tau, h))$ and entangling power (bottom) when $h_x^i = 1.0$, $h_y^i = 0$, $h_z^i = 1$, and $\tau = \pi/4$. The nonintegrable case Set-NI is shown in the latter figure for comparison.

terms of fermions, it promises to be an interesting one for further studies.

IV. SUMMARY AND CONCLUSIONS

In this paper, we have studied the growth and saturation of operator entanglement entropy and entangling power of time evolution operators of a kicked Ising spin chain for both integrable and non-integrable configurations. These quantities have been studied with respect to both linear and von Neumann entropies. We have analytically solved for the operator entanglement entropies and the linear entropy entangling power for the integrable configuration. The growth and saturation of these quantities have also been compared with that obtained from a hybrid random matrix model which replaces the block of $L/2$ spins between which entanglement is found by a random operator.

In the case of the integrable model, referred to as set-I, we have found a precise linear growth of operator von Neumann entanglement entropy and an exponential growth of linear entropy entangling power. Interestingly, the nonintegrable model also shows the same growth for the operator entanglement entropy. However, on looking at the entangling power we see that it increases only over $L/2$ kicks for the integrable model while for the nonintegrable model it continues to increase and saturates at a significantly higher value after L kicks. The random matrix model for which we can find the linear entropy entangling power exactly, reproduces the nonintegrable curves rather well. However, we also find that that certain nonintegrable models with the Wigner distribution of NNS does not match the entangling power from the random matrix model that well. This leads us to the study of long-range spectral correlations such as number-variance, which shows differences amongst these nonintegrable cases. This implies that long-range correlations that affect short-time behaviors are important in understanding the growth of entanglement in these systems than simply the NNS alone. Finally, we have displayed an interesting configuration which, while being an interacting model in terms of Jordan-Wigner fermions, show a periodic increase and decrease of operator entanglement entropy with number of kicks. The entangling power of the model, while still periodic, reaches a maximum value equal to the saturation value of the nonintegrable model studied previously.

Relying on analytical and numerical RMT averages for bipartite entangling powers, we have seen that while it sometimes describes very well the time evolution of such measures, it mostly provides an upper bound for other nonintegrable situations. Thus, one outstanding work is to find entangling power in random circuits that take into account the internal structure of local blocks and may provide better estimates in other cases. The measures studied in this paper are primarily entanglement-based ones. It will be interesting to explore connections with other measures such as operator spreading [45] and how the operator entanglement of an initially local operator changes with time in the Heisenberg picture [23]. We have also seen how the increased multipartite entanglement produced in nonintegrable evolutions, in comparison with integrable ones, plays a role in the growth of entangling power. Thus, notions of entangling capabilities based on multiparty entanglement measures such as tripartite mutual information [46] promises to be an interesting one. There may also be interesting connections to scrambling and growth of out-of-time-ordered-correlators [46]. There has also been recently a series of studies on the spectral form factor, which is the Fourier transform of two-point correlation of the eigenvalue density of the time-evolution operator, in the kicked Ising and random circuit models [47,48]. Our findings are consistent with these results and complements them as number variance and form factor are related [49].

ACKNOWLEDGMENT

R.P. would like to gratefully acknowledge Ravi Prakash for useful discussions and help with computing the number variance.

APPENDIX A: ANTIUNITARY SYMMETRY AND FALSE TIME REVERSAL

Suppose the system has an antiunitary symmetry governed by $T = G\,K$, where K is the complex conjugation operator and G is unitary. The condition that time-reversal-like symmetry holds for a system whose time evolution is the unitary operator U, is [2]

$$T\,U\,T^{-1} = U^{-1} = U^{\dagger},$$

implying that

$$GU^{*}G^{-1} = U^{\dagger}. \tag{A1}$$

For our model, we have

$$U^* = \exp\left(i\tau\left(\sum_{j=1}^{L-1}\sigma_j^z\sigma_{j+1}^z + \sum_{j=1}^{L}h_i^z\sigma_i^z\right)\right) \times \exp\left(i\tau\sum_{j=1}^{L}\left(h_j^x\sigma_j^x - h_j^y\sigma_j^y\right)\right)$$

and

$$U^\dagger = \exp\left(i\tau\sum_{j=1}^{L}\left(h_j^x\sigma_j^x + h_j^y\sigma_j^y\right)\right) \times \exp\left(i\tau\left(\sum_{j=1}^{L-1}\sigma_j^z\sigma_{j+1}^z + \sum_{j=1}^{L}h_i^z\sigma_i^z\right)\right).$$

For $h_j^y = 0$, for all j, clearly

$$G_1 = \exp\left(-i\tau\left(\sum_{j=1}^{L-1}\sigma_j^z\sigma_{j+1}^z + \sum_{j=1}^{L}h_i^z\sigma_i^z\right)\right)$$

satisfies Eq. (A1).

We have

$$G_1U^*G_1^{-1} = \exp\left(i\tau\sum_{j=1}^{L}\left(h_j^x\sigma_j^x - h_j^y\sigma_j^y\right)\right) \times \exp\left(i\tau\left(\sum_{j=1}^{L-1}\sigma_j^z\sigma_{j+1}^z + \sum_{j=1}^{L}h_i^z\sigma_i^z\right)\right).$$

Let $h_j^x\,\hat{x} - h_j^y\,\hat{y} = h_j(\cos(\theta_j)\hat{x} - \sin(\theta_j)\hat{y}) = h_j\hat{h_j}$ and $V_j = \exp(-i\sigma_j^z\theta_j)$ be a spin rotation operator, performing the rotation $2\theta_j$ about z axis so that we have

$$V_j\left(\cos(\theta_j)\sigma_j^x - \sin(\theta_j)\sigma_j^y\right)V_j^\dagger = \left(\cos(\theta_j)\sigma_j^x + \sin(\theta_j)\sigma_j^y\right),$$

$[V_j, \sigma_j^z] = 0$.

It follows that

$$V_j\exp\left(i\tau\left(h_j^x\sigma_j^x - h_j^y\sigma_j^y\right)\right)V_j^\dagger = \exp\left(i\tau\left(h_j^x\sigma_j^x + h_j^y\sigma_j^y\right)\right). \tag{A2}$$

Hence, with

$$G = \left(\bigotimes_{j=1}^{L}V_j\right)G_1,$$

Equation (A1) is satisfied for the Floquet operator. This implies COE statistics as we have shown, and is valid for all disordered models as well.

APPENDIX B: PROOF OF $E_l(U^nS) = 1 - \frac{2^{n-1}}{2^L}$.

To find $E_l(U^nS)$, we will work in the ancilla picture mentioned in Sec. II A, as the combinatorics involved is easier to see in terms of states rather than operators. The ancilla picture would require us to consider a four-party state with the dimension of each party being $N = 2^{L/2}$. Together with the original spin chain with spins indexed by A_i and B_j according to the notation explained before, we consider an ancillary spin chain of same length with sites labeled by A_i' and B_j' ($i, j = 1..L/2$), see Fig. 10. We will be interested in the state

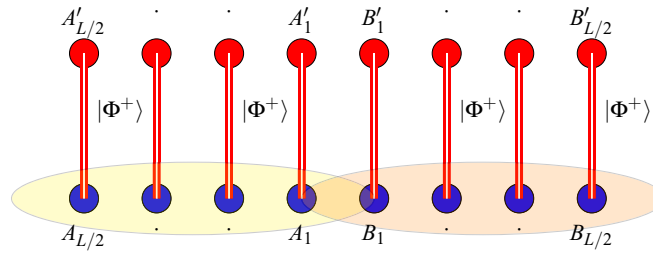

FIG. 10. Ancilla picture for the spin chain: the spins in the lower row are subjected to the spin chain dynamics while the upper (ancilla) are not. Initially, corresponding pairs of spins between the chain and the ancilla are maximally entangled in a Bell state $|\Phi^+\rangle$. To find the operator entanglement of U^nS, one needs to find the entanglement across the $A_1A_1'..A_{L/2}A_{L/2}'$ and $B_1B_1'..B_{L/2}B_{L/2}'$ bipartition of the state obtained by the action of U^nS on the $A_1A_2..A_{L/2}B_1B_2..B_{L/2}$ subsystem.

$$|\Phi\rangle_{ABA'B'} = \bigotimes_{i=1}^{L/2}|\Phi^+\rangle_{A_iA_i'}|\Phi^+\rangle_{B_iB_i'},$$

where $|\Phi^+\rangle$ is one of the Bell states:

$$|\Phi^\pm\rangle = \frac{1}{\sqrt{2}}(|00\rangle \pm |11\rangle), \quad |\Psi^\pm\rangle = \frac{1}{\sqrt{2}}(|01\rangle \pm |10\rangle).$$

The linear $E_l(U^n\,S)$ is the linear entropy of the state, $((U^nS)_{AB}\otimes I_{A'B'})|\Phi\rangle_{ABA'B'}$, across the $AA'|BB'$ partitions. Notice that the swap operation has been clubbed along with the unitary evolution in this setting. Also it is sufficient here to consider only the nonlocal part $(U^n)_{nl}$ part of U^n.

We have

$$((U^n)_{nl}\,S)_{AB}\otimes I_{A'B'})|\Phi\rangle_{ABA'B'} = \prod_{i=1}^{n}V_i\prod_{j=1}^{L/2}S_{jj}\bigotimes_{j=1}^{L/2}|\Phi^+\rangle_{A_jA_j'}|\Phi^+\rangle_{B_jB_j'},$$

where we have use that

$$S = \prod_{j=1}^{L/2}S_{jj}, \quad \text{with} \quad S_{ii} \equiv S_{A_iB_i}$$

are swap operators on pairs of spins in the different partitions. Their action on the bell pairs yield

$$S_{ii}|\Phi^+\rangle_{A_iA_i'}|\Phi^+\rangle_{B_iB_i'} = |\Phi^+\rangle_{A_iB_i'}|\Phi^+\rangle_{A_i'B_i} \equiv |\alpha\rangle_i, \tag{B1}$$

which has two ebits of entanglement (Schmidt rank-4 state) across the $A_iA_i'|B_iB_i'$ partition. It is thus clear that $|\alpha\rangle_1\cdots|\alpha\rangle_n$ will be a maximally entangled state in 4^n ($2n$ ebits) dimensions. Particularly, for $n = L/2$ we will have $E_l(S) = 1 - 1/2^L = 1 - 1/N^2$. We need $E_l(U^nS)$, which is the linear entropy of the state $\prod_{i=1}^{n}V_i\bigotimes_{j=1}^{L/2}|\alpha\rangle_j$.

Our basic strategy will consist of showing that the entanglement of the state $\prod_{i=1}^{n} V_i \bigotimes_{j=1}^{n} |\alpha\rangle_j$ grows as $n+1$ ebits for $n \leqslant L/2$. On the other hand, $\bigotimes_{i=n+1}^{L/2} |\alpha\rangle_i$ will contribute $L-2n$ ebits, so that totally we have $L-n+1$ ebits. This will imply $E_l(U^n S) = 1 - 2^{n-1}/2^L$. This together with the result for $E_l(U^n)$ proved before yields the desired result. For $n = L/2+m$ ($m < L/2$), we will adopt the same strategy as for $E_l(U^n)$ for $n > L/2$ and define V' operators. Then we would try to find the entanglement in the state, $\prod_{j=1}^{\frac{L}{2}-m} V_j \prod_{l=1}^{m} V'_l |\alpha\rangle_1 |\alpha\rangle_2 ... |\alpha\rangle_{\frac{L}{2}}$. It will turn out that this is in fact equal to the entanglement in the state $\prod_{j=1}^{\frac{L}{2}-m} V_j |\alpha\rangle_1 |\alpha\rangle_2 ... |\alpha\rangle_{\frac{L}{2}-m} = L/2 - m + 1$ ebits $= L - n + 1$ ebits.

We state the following readily verifiable identities for later use:

$$\begin{aligned} A_i^x B_i^x |\Phi^+\rangle_{A_i B_i'} |\Phi^+\rangle_{A_i' B_i} &= |\Psi^+\rangle_{A_i B_i'} |\Psi^+\rangle_{A_i' B_i}, \\ A_i^y B_i^y |\Phi^+\rangle_{A_i B_i'} |\Phi^+\rangle_{A_i' B_i} &= |\Psi^-\rangle_{A_i B_i'} |\Psi^-\rangle_{A_i' B_i}, \\ A_i^z B_i^z |\Phi^+\rangle_{A_i B_i'} |\Phi^+\rangle_{A_i' B_i} &= |\Phi^-\rangle_{A_i B_i'} |\Phi^-\rangle_{A_i' B_i}. \end{aligned} \tag{B2}$$

$$\begin{aligned} |\Phi^+\rangle_{A_1 B_1'} |\Phi^+\rangle_{A_1' B_1} + |\Psi^-\rangle_{A_1 B_1'} |\Psi^-\rangle_{A_1' B_1} &= |\Phi^+\rangle_{A_1 A_1'} |\Phi^+\rangle_{B_1 B_1'} - |\Psi^-\rangle_{A_1 A_1'} |\Psi^-\rangle_{B_1 B_1'}, \\ |\Phi^+\rangle_{A_1 B_1'} |\Phi^+\rangle_{A_1' B_1} - |\Psi^-\rangle_{A_1 B_1'} |\Psi^-\rangle_{A_1' B_1} &= |\Phi^-\rangle_{A_1 A_1'} |\Phi^-\rangle_{B_1 B_1'} + |\Psi^+\rangle_{A_1 A_1'} |\Psi^+\rangle_{B_1 B_1'}, \\ |\Psi^+\rangle_{A_1 B_1'} |\Psi^+\rangle_{A_1' B_1} + |\Phi^-\rangle_{A_1 B_1'} |\Phi^-\rangle_{A_1' B_1} &= |\Phi^+\rangle_{A_1 A_1'} |\Phi^+\rangle_{B_1 B_1'} + |\Psi^-\rangle_{A_1 A_1'} |\Psi^-\rangle_{B_1 B_1'}, \\ |\Psi^+\rangle_{A_1 B_1'} |\Psi^+\rangle_{A_1' B_1} - |\Phi^-\rangle_{A_1 B_1'} |\Phi^-\rangle_{A_1' B_1} &= |\Psi^+\rangle_{A_1 A_1'} |\Psi^+\rangle_{B_1 B_1'} - |\Phi^-\rangle_{A_1 A_1'} |\Phi^-\rangle_{B_1 B_1'}. \end{aligned} \tag{B3}$$

Let $\tilde{A}_K$ and $\tilde{B}_K$ represent the following collection of spins:

$$\begin{aligned} \tilde{A}_K &\equiv \{A_1, A_1', \cdots, A_K, A_K'\}, \\ \tilde{B}_K &\equiv \{B_1, B_1', \cdots B_K, B_K'\}, \end{aligned}$$

and $C(n) = \prod_{k=1}^{n} A_k^x B_k^x$ be the string of operators. We have

Lemma 1.

(1) $V_1|\alpha\rangle_1$ has a Schmidt decomposition,

$$\begin{aligned} &\tfrac{1}{2}\big(|00\rangle_{A_1 A_1'} |\Phi'^-\rangle_{B_1 B_1'} + i|01\rangle_{A_1 A_1'} |\Psi'^-\rangle_{B_1 B_1'} \\ &\quad + |10\rangle_{A_1 A_1'} |\Psi'^+\rangle_{B_1 B_1'} - i|11\rangle_{A_1 A_1'} |\Phi'^+\rangle_{B_1 B_1'}\big), \end{aligned}$$

with $|\Phi'^{\pm}\rangle = \frac{1}{\sqrt{2}}(|00\rangle \pm i|11\rangle)$ and $|\Psi'^{\pm}\rangle = \frac{1}{\sqrt{2}}(|01\rangle \pm i|10\rangle)$. This can also be written in terms of biorthogonal vectors as

$$\frac{1}{2}\sum_{i=1}^{2} (|e_i\rangle_{\tilde{A}_1 \tilde{B}_1} + |e_i'\rangle_{\tilde{A}_1 \tilde{B}_1}),$$

so that $|e_i'\rangle_{\tilde{A}_1 \tilde{B}_1} = i\, C(1) |e_i\rangle_{\tilde{A}_1 \tilde{B}_1}$, where $|e_1\rangle_{\tilde{A}_1 \tilde{B}_1} = |00\rangle_{A_1 A_1'} |\Phi'^-\rangle_{B_1 B_1'}$ and $|e_2\rangle_{\tilde{A}_1 \tilde{B}_1} = -i|11\rangle_{A_1 A_1'} |\Phi'^+\rangle_{B_1 B_1'}$.

(2) $E_l(US) = E_l(S)$

Proof. The first part follows from direct computations. We state the following useful identities:

$$(\sigma_x \otimes I)|\Phi'^{\pm}\rangle = \pm i |\Psi'^{\mp}\rangle, \quad (\sigma_x \otimes I)|\Psi'^{\pm}\rangle = \pm i |\Phi'^{\mp}\rangle, \tag{B4}$$

and observe

$$\begin{aligned} i|01\rangle_{A_1 A_1'} |\Psi'^-\rangle_{B_1 B_1'} &= i\, C(1)\, (-i|11\rangle_{A_1 A_1'} |\Phi'^+\rangle_{B_1 B_1'}), \\ |10\rangle_{A_1 A_1'} |\Psi'^+\rangle_{B_1 B_1'} &= i\, C(1) |00\rangle_{A_1 A_1'} |\Phi'^-\rangle_{B_1 B_1'}. \end{aligned}$$

The second part follows as a consequence, as $V_1|\alpha\rangle_1$ is a rank-4 maximal Schmidt decomposition, the same as $|\alpha\rangle_1$. The von Neumann entanglement in these states is two ebits.

We are now ready to prove the main lemma.

Lemma 2.

The von Neumann entropy of $\prod_{i=1}^{n} V_i \bigotimes_{j=1}^{n} |\alpha\rangle_j$ is $= n+1$, $1 \leqslant n \leqslant L/2$.

Proof.

The proof is inductive. Let us first analyze, $V_2 V_1 |\alpha\rangle_1 |\alpha\rangle_2$. On expanding V_2 and using Eq. (B2), we have

$$\begin{aligned} V_2 V_1 |\alpha\rangle_1 |\alpha\rangle_2 = \frac{1}{\sqrt{2}} &(V_1 |\alpha\rangle_1 |\Phi^+\rangle_{A_2 B_2'} |\Phi^+\rangle_{A_2' B_2} \\ &- i\, C(1) V_1 |\alpha\rangle_1 |\Psi^-\rangle_{A_2 B_2'} |\Psi^-\rangle_{A_2' B_2}). \end{aligned}$$

Let us now use the lemma above and consider the contribution from the term $|e_i\rangle_{\tilde{A}_1 \tilde{B}_1} + |e_i'\rangle_{\tilde{A}_1 \tilde{B}_1}$, to the Schmidt decomposition of $V_2 V_1 |\alpha\rangle_1 |\alpha\rangle_2$ for different i. We have on using $C(1)^2 = I$,

$$\begin{aligned} V_2 V_1 |\alpha\rangle_1 |\alpha\rangle_2 = \frac{1}{2\sqrt{2}} \sum_{i=1,2} [&|e_i\rangle_{\tilde{A}_1 \tilde{B}_1} (|\Phi^+\rangle_{A_2 B_2'} |\Phi^+\rangle_{A_2' B_2} \\ &+ |\Psi^-\rangle_{A_2 B_2'} |\Psi^-\rangle_{A_2' B_2}) + |e_i'\rangle_{\tilde{A}_1 \tilde{B}_1} \\ &\times (|\Phi^+\rangle_{A_2 B_2'} |\Phi^+\rangle_{A_2' B_2} - |\Psi^-\rangle_{A_2 B_2'} |\Psi^-\rangle_{A_2' B_2})] \end{aligned}$$

Using Eq. (B3), we rewrite the state so that the partition $AA'|BB'$ or $\tilde{A}_2|\tilde{B}_2$ can be read off:

$$\begin{aligned} &V_2 V_1 |\alpha\rangle_1 |\alpha\rangle_2 \\ &= \frac{1}{2\sqrt{2}} \sum_{i=1,2} (|e_i\rangle_{\tilde{A}_1 \tilde{B}_1} (|\Phi^+\rangle_{A_2 A_2'} |\Phi^+\rangle_{B_2 B_2'} \\ &\quad - |\Psi^-\rangle_{A_2 A_2'} |\Psi^-\rangle_{B_2 B_2'}) + |e_i'\rangle_{\tilde{A}_1 \tilde{B}_1} (|\Phi^-\rangle_{A_2 A_2'} |\Phi^-\rangle_{B_2 B_2'} \\ &\quad + |\Psi^+\rangle_{A_2 A_2'} |\Psi^+\rangle_{B_2 B_2'}). \end{aligned}$$

We started with a Schmidt decomposition of $V_1|\alpha\rangle_1$, and clearly the above is also Schmidt decomposed across the $A_1 A_2 A_1' A_2' | B_1 B_2 B_1' B_2'$ or $\tilde{A}_2 | \tilde{B}_2$ partition. It is maximally entangled in an *eight*-dimensional subspace of the 16-dimensional space. Hence, its von Neumann entropy is three ebits.

A crucial observation is that with suitable definitions this can be written as

$$V_2V_1|\alpha\rangle_1|\alpha\rangle_2 = \frac{1}{2\sqrt{2}}\left(\sum_{i=1}^{4}|e_i\rangle_{\tilde{A}_2\tilde{B}_2} + |e_i'\rangle_{\tilde{A}_2\tilde{B}_2}\right),$$

where for $i = 1, 2$,

$$\begin{aligned}
|e_i'\rangle_{\tilde{A}_2\tilde{B}_2} &= |e_i'\rangle_{\tilde{A}_1\tilde{B}_1}|\Psi^+\rangle_{A_2A_2'}|\Psi^+\rangle_{B_2B_2'},\\
|e_i\rangle_{\tilde{A}_2\tilde{B}_2} &= |e_i\rangle_{\tilde{A}_1\tilde{B}_1}|\Phi^+\rangle_{A_2A_2'}|\Phi^+\rangle_{B_2B_2'},\\
|e_{i+2}'\rangle_{\tilde{A}_2\tilde{B}_2} &= -|e_i\rangle_{\tilde{A}_1\tilde{B}_1}|\Psi^-\rangle_{A_2A_2'}|\Psi^-\rangle_{B_2B_2'},\\
|e_{i+2}\rangle_{\tilde{A}_2\tilde{B}_2} &= |e_i'\rangle_{\tilde{A}_1\tilde{B}_1}|\Phi^-\rangle_{A_2A_2'}|\Phi^-\rangle_{B_2B_2'}.
\end{aligned}$$

These satisfy $|e_i'\rangle_{\tilde{A}_2\tilde{B}_2} = i\,C(2)|e_i\rangle_{\tilde{A}_2\tilde{B}_2}$, for $1 \leqslant i \leqslant 4$ and this is exactly the relation between the Schmidt vectors at level 1. Note that these continue to be biorthogonal and is therefore indeed a Schmidt decomposition.

Now, assume a Schmidt decomposition of rank 2^n of

$$\begin{aligned}
&\left(\prod_{i=1}^{n-1}V_i\right)|\alpha\rangle_1|\alpha\rangle_2...|\alpha\rangle_{n-1}\\
&\quad= \frac{1}{2^{n/2}}\left(\sum_{i=1}^{2^{n-1}}(|e_i\rangle_{\tilde{A}_{n-1}\tilde{B}_{n-1}} + |e_i'\rangle_{\tilde{A}_{n-1}\tilde{B}_{n-1}})\right),
\end{aligned}$$

with $|e_i'\rangle_{\tilde{A}_{n-1}\tilde{B}_{n-1}} = iC(n-1)|e_i\rangle_{\tilde{A}_{n-1}\tilde{B}_{n-1}}$.

Following the same steps as the first level, we get

$$\begin{aligned}
\prod_{i=1}^{n}V_i\bigotimes_{j=1}^{n}|\alpha\rangle_j = \frac{1}{2^{(n+1)/2}}\sum_{i=1}^{2^{n-1}}&(|e_i\rangle_{\tilde{A}_{n-1}\tilde{B}_{n-1}}(|\Phi^+\rangle_{A_nA_n'}|\Phi^+\rangle_{B_nB_n'}\\
&- |\Psi^-\rangle_{A_nA_n'}|\Psi^-\rangle_{B_nB_n'})\\
&+ |e_i'\rangle_{\tilde{A}_{n-1}\tilde{B}_{n-1}}(|\Phi^-\rangle_{A_nA_n'}|\Phi^-\rangle_{B_nB_n'}\\
&+ |\Psi^+\rangle_{A_nA_n'}|\Psi^+\rangle_{B_nB_n'})),
\end{aligned}$$

which can also be written in Schmdit decomposed form using biorthogonal vectors as

$$\frac{1}{2^{(n+1)/2}}\left(\sum_{i=1}^{2^n}(|e_i\rangle_{\tilde{A}_n\tilde{B}_n} + |e_i'\rangle_{\tilde{A}_n\tilde{B}_n})\right), \tag{B5}$$

where, for $1 \leqslant i \leqslant 2^{n-1}$,

$$\begin{aligned}
|e_i'\rangle_{\tilde{A}_n\tilde{B}_n} &= |e_i'\rangle_{\tilde{A}_{n-1}\tilde{B}_{n-1}}|\Psi^+\rangle_{A_nA_n'}|\Psi^+\rangle_{B_nB_n'},\\
|e_i\rangle_{\tilde{A}_n\tilde{B}_n} &= |e_i\rangle_{\tilde{A}_{n-1}\tilde{B}_{n-1}}|\Phi^+\rangle_{A_nA_n'}|\Phi^+\rangle_{B_nB_n'},\\
|e_{i+2^{n-1}}'\rangle_{\tilde{A}_n\tilde{B}_n} &= -|e_i\rangle_{\tilde{A}_{n-1}\tilde{B}_{n-1}}|\Psi^-\rangle_{A_nA_n'}|\Psi^-\rangle_{B_nB_n'},\\
|e_{i+2^{n-1}}\rangle_{\tilde{A}_n\tilde{B}_n} &= |e_i'\rangle_{\tilde{A}_{n-1}\tilde{B}_{n-1}}|\Phi^-\rangle_{A_nA_n'}|\Phi^-\rangle_{B_nB_n'}.
\end{aligned}$$

These satisfy $|e_i'\rangle_{\tilde{A}_n\tilde{B}_n} = i\,C(n)|e_i\rangle_{\tilde{A}_n\tilde{B}_n}$, for $1 \leqslant i \leqslant 2^n$, the same relation at the previous levels. Thus, it follows that the von Neumann entropy of $\prod_{i=1}^{n}V_i|\alpha\rangle_1|\alpha\rangle_2...|\alpha\rangle_n$ is $n+1$.

Lemma 3. The von Neumann entropy of the state $\prod_{j=1}^{\frac{L}{2}+m}V_j|\alpha\rangle_1|\alpha\rangle_2...|\alpha\rangle_{\frac{L}{2}})$ is equal to the von Neumann entropy of the state $|\beta_m\rangle \equiv \prod_{j=1}^{\frac{L}{2}-m}V_j|\alpha\rangle_1|\alpha\rangle_2...|\alpha\rangle_{\frac{L}{2}-m}$, for $1 \leqslant m < L/2$.

Proof.

We use again the strategy of pairing the V_j operators beyond $j = L/2 - m$ into $V'_{m+1-k} = V_{L/2-k+1}V_{L/2+k}$. Denote $n_2 = n_1 + 1 = L/2 - m + 1$, and in all expressions $1 \leqslant m < L/2$. For example,

$$\begin{aligned}
V_1' = V_{\frac{L}{2}-m+1}V_{\frac{L}{2}+m} = \tfrac{1}{2}\big(&I - iA^z_{n_2}B^z_{n_2}C(n_1)\\
&- iA^y_{n_2}B^y_{n_2}C(n_1) + A^x_{n_2}B^x_{n_2}\big).
\end{aligned}$$

Direct computation and the usage of identities in Eq. (B3) results in

$$\begin{aligned}
&V_1'|\beta_m\rangle|\alpha\rangle_{n_2}\\
&\quad= \frac{1}{2^{(n_1+1)/2}}\sum_{i=1}^{2^{n_1}}\big(|e_i\rangle_{\tilde{A}_{n_1}\tilde{B}_{n_1}}|\Phi^+\rangle_{A_{n_2}B'_{n_2}}|\Phi^+\rangle_{A'_{n_2}B_{n_2}}\\
&\qquad+ |e_i'\rangle_{\tilde{A}_{n_1}\tilde{B}_{n_1}}|\Psi^+\rangle_{A_{n_2}B'_{n_2}}|\Psi^+\rangle_{A'_{n_2}B_{n_2}}\big).
\end{aligned}$$

As previously, we have

$$\begin{aligned}
&|e_i'\rangle_{\tilde{A}_{n_1}\tilde{B}_{n_1}}|\Psi^+\rangle_{A_{n_2}B'_{n_2}}|\Psi^+\rangle_{A'_{n_2}B_{n_2}}\\
&\quad= iC(n_2)|e_i\rangle_{\tilde{A}_{n_1}\tilde{B}_{n_1}}|\Phi^+\rangle_{A_{n_2}B'_{n_2}}|\Phi^+\rangle_{A'_{n_2}B_{n_2}}.
\end{aligned}$$

But note that $|\beta_m\rangle$ is also in Eq. (B5) with $n = n_1 = L/2 - m$. Hence, $V_1'|\beta_m\rangle|\alpha\rangle_{n_1+1}$ has the same entanglement as $|\beta_m\rangle$. Now, assuming $\prod_{l=1}^{k}V_l'|\beta_m\rangle|\alpha\rangle_{n_1+1}|\alpha\rangle_{n_1+2}..|\alpha\rangle_{n_1+k}$ has the same entanglement as $|\beta_m\rangle$ $(k \leqslant m)$, it is easy to show by following the same steps that $\prod_{l=1}^{k+1}V_l'|\beta_m\rangle|\alpha\rangle_{n_1+1}|\alpha\rangle_{n_1+2}..|\alpha\rangle_{n_1+k+1}$ also has the same entanglement. Hence, the lemma follows by induction.

Lemma 4. For $1 \leqslant n \leqslant L$, the linear operator entanglement entropy is $E_l(U^nS) = 1 - 2^{-L+n-1}$.

Proof. Let us denote the von Neumann entropy of a state $|\cdot\rangle$, by $\mathscr{E}_{vn}(|\cdot\rangle)$. For $n \leqslant L/2$, by Lemma 2,

$$\mathscr{E}_{vn}\left(\prod_{i=1}^{n}V_i\bigotimes_{j=1}^{n}|\alpha\rangle_j\right) = n+1.$$

We also have

$$\mathscr{E}_{vn}\left(\bigotimes_{i=n+1}^{L/2}|\alpha\rangle_i\right) = 2\,(L/2-n) = L-2n.$$

Hence,

$$\begin{aligned}
\mathscr{E}_{vn}\left(\prod_{i=1}^{n}V_i\bigotimes_{j=1}^{n}|\alpha\rangle_j\bigotimes_{i=n+1}^{L/2}|\alpha\rangle_i\right) &= (L-2n)+(n+1)\\
&= L-n+1.
\end{aligned} \tag{B6}$$

As the Schmdit decompositions are all maximal, the linear operator entanglement is

$$E_l(U^nS) = 1 - \frac{1}{2^{(L-n+1)}} = 1 - \frac{2^{n-1}}{2^L}. \tag{B7}$$

For times larger than $n = L/2$, consider $L/2 < n < L$, and let $m = n - L/2$. It follows from Lemma 3 that

$$\mathscr{E}_{vn}\left(\prod_{j=1}^{\frac{L}{2}+m} V_j|\alpha\rangle_1|\alpha\rangle_2 ...|\alpha\rangle_{\frac{L}{2}}\right) = L/2 - m + 1 = L - n + 1. \tag{B8}$$

Hence, Eq. (B7) continues to hold. We still have one more time $n = L$ to cover and this needs special treatment. We need to find

$$\mathscr{E}_{vn}\left(\prod_{l=1}^{L/2} V_l' \bigotimes_{j=1}^{L/2} |\alpha\rangle_j\right).$$

By direct, but tedious, computation it follows that

$$V_1'|\alpha\rangle_1 = \frac{1}{\sqrt{2}}\left(\frac{(1-i)}{\sqrt{2}}|\Phi^+\rangle_{A_1A_1'}|\Phi^+\rangle_{B_1B_1'} + \frac{(1+i)}{\sqrt{2}}|\Psi^+\rangle_{A_1A_1'}|\Psi^+\rangle_{B_1B_1'}\right)$$

and

$$\frac{(1+i)}{\sqrt{2}}|\Psi^+\rangle_{A_1A_1'}|\Psi^+\rangle_{B_1B_1'} = iA_1^xB_1^x\frac{(1-i)}{\sqrt{2}}|\Phi^+\rangle_{A_1A_1'}|\Phi^+\rangle_{B_1B_1'}.$$

Hence, following the same steps as in the proof of Lemma 3, it is straightforward to see that

$$\mathscr{E}_{vn}\left(\prod_{l=1}^{L/2} V_l' \bigotimes_{j=1}^{L/2} |\alpha\rangle_j\right) = \mathscr{E}_{vn}(V_1'|\alpha\rangle_1) = 1.$$

Thus, Eq. (B8) holds uniformly for $1 \leqslant n \leqslant L$. In particular, note that it decreases from L initially ($n = 0$) and at $n = 1$ to 1 at $n = L$. This precipitous fall makes up for the rise of the operator entanglement of U^n. This also completes the proof of the lemma.

For $n \geqslant L$, we again use the fact that U^{2L} is a local operator. We have $E_l(U^{2L-m}S) = E_l(U^{-m}S) = E_l(U^mS)$. Now, putting $m = L - m$, we have $E_l(U^{L-m}S) = E_l(U^{L+m}S)$.

[1] M. Berry, Quantum chaology, not quantum chaos, Phys. Scr. **40**, 335 (1989).

[2] F. Haake, *Quantum Signatures of Chaos* (Springer, Berlin, Heidelberg,2010).

[3] M. C. Gutzwiller, *Chaos in Classical and Quantum Mechanics* (Springer-Verlag, New York, 1990).

[4] L. D'Alessio, Y. Kafri, A. Polkovnikov, and M. Rigol, From quantum chaos and eigenstate thermalization to statistical mechanics and thermodynamics, Adv. Phys. **65**, 239 (2016).

[5] J. A. Kjäll, J. H. Bardarson, and F. Pollmann, Many-Body Localization in a Disordered Quantum Ising Chain, Phys. Rev. Lett. **113**, 107204 (2014).

[6] D. A. Roberts, D. Stanford, and L. Susskind, Localized shocks, J. High Energy Phys. 03 (2015) 051.

[7] B. Swingle, G. Bentsen, M. Schleier-Smith, and P. Hayden, Measuring the scrambling of quantum information, Phys. Rev. A **94**, 040302 (2016).

[8] I. Kukuljan, S. Grozdanov, and T. Prosen, Weak quantum chaos, Phys. Rev. B **96**, 060301 (2017).

[9] D. J. Luitz and Y. Bar Lev, Information propagation in isolated quantum systems, Phys. Rev. B **96**, 020406(R) (2017).

[10] R. Horodecki, P. Horodecki, M. Horodecki, and K. Horodecki, Quantum entanglement, Rev. Mod. Phys. **81**, 865 (2009).

[11] L. Amico, R. Fazio, A. Osterloh, and V. Vedral, Entanglement in many-body systems, Rev. Mod. Phys. **80**, 517 (2008).

[12] Z.-C. Yang, A. Hamma, S. M. Giampaolo, E. R. Mucciolo, and C. Chamon, Entanglement complexity in quantum many-body dynamics, thermalization, and localization, Phys. Rev. B **96**, 020408 (2017).

[13] P. A. Miller and S. Sarkar, Signatures of chaos in the entanglement of two coupled quantum kicked tops, Phys. Rev. E **60**, 1542 (1999).

[14] J. N. Bandyopadhyay and A. Lakshminarayan, Testing Statistical Bounds on Entanglement Using Quantum Chaos, Phys. Rev. Lett. **89**, 060402 (2002).

[15] J. Eisert, M. Cramer, and M. B. Plenio, Colloquium, Rev. Mod. Phys. **82**, 277 (2010).

[16] S. Montangero and L. Viola, Multipartite entanglement generation and fidelity decay in disordered qubit systems, Phys. Rev. A **73**, 040302 (2006).

[17] A. Nahum, J. Ruhman, S. Vijay, and J. Haah, Quantum Entanglement Growth Under Random Unitary Dynamics, Phys. Rev. X **7**, 031016 (2017).

[18] K. Najafi, M. A. Rajabpour, and J. Viti, Light-cone velocities after a global quench in a noninteracting model, Phys. Rev. B **97**, 205103 (2018).

[19] T. Prosen, Chaos and complexity of quantum motion, J. Phys. A **40**, 7881 (2007).

[20] P. Calabrese and J. Cardy, Evolution of entanglement entropy in one-dimensional systems, J. Stat. Mech. (2005) P04010.

[21] H. Kim and D. A. Huse, Ballistic Spreading of Entanglement in a Diffusive Nonintegrable System, Phys. Rev. Lett. **111**, 127205 (2013).

[22] T. Zhou and D. J. Luitz, Operator entanglement entropy of the time evolution operator in chaotic systems, Phys. Rev. B **95**, 094206 (2017).

[23] J. Dubail, Entanglement scaling of operators: a conformal field theory approach, with a glimpse of simulability of long-time dynamics in $1+1d$, J. Phys. A **50**, 234001 (2017).

[24] P. Zanardi, C. Zalka, and L. Faoro, Entangling power of quantum evolutions, Phys. Rev. A **62**, 030301 (2000).

[25] P. Zanardi, Entanglement of quantum evolutions, Phys. Rev. A **63**, 040304 (2001).

[26] M. A. Nielsen, C. M. Dawson, J. L. Dodd, A. Gilchrist, D. Mortimer, T. J. Osborne, M. J. Bremner, A. W. Harrow, and A. Hines, Quantum dynamics as a physical resource, Phys. Rev. A **67**, 052301 (2003).

[27] F. Caruso, A. W. Chin, A. Datta, S. F. Huelga, and M. B. Plenio, Entanglement and entangling power of the dynamics in light-harvesting complexes, Phys. Rev. A **81**, 062346 (2010).

[28] R. Demkowicz-Dobrzański and M. Kuś, Global entangling properties of the coupled kicked tops, Phys. Rev. E **70**, 066216 (2004).

[29] F. A. Calderon-Vargas and J. P. Kestner, Entanglement dynamics of two Ising-coupled qubits with nonperpendicular local driving fields, Phys. Rev. B **97**, 125311 (2018).

[30] A. Lakshminarayan and V. Subrahmanyam, Multipartite entanglement in a one-dimensional time-dependent Ising model, Phys. Rev. A **71**, 062334 (2005).

[31] A. J. Scott and C. M. Caves, Entangling power of the quantum baker's map, J. Phys. A **36**, 9553 (2003).

[32] X. Wang, B. C. Sanders, and D. W. Berry, Entangling power and operator entanglement in qudit systems, Phys. Rev. A **67**, 042323 (2003).

[33] B. Jonnadula, P. Mandayam, K. Życzkowski, and A. Lakshminarayan, Impact of local dynamics on entangling power, Phys. Rev. A **95**, 040302 (2017).

[34] M. Musz, M. Kuś, and K. Życzkowski, Unitary quantum gates, perfect entanglers, and unistochastic maps, Phys. Rev. A **87**, 022111 (2013).

[35] D. N. Page, Average Entropy of a Subsystem, Phys. Rev. Lett. **71**, 1291 (1993).

[36] S. C. L. Srivastava, S. Tomsovic, A. Lakshminarayan, R. Ketzmerick, and A. Bäcker, Universal Scaling of Spectral Fluctuationtransitions for Interacting Chaotic Systems, Phys. Rev. Lett. **116**, 054101 (2016).

[37] A. Lakshminarayan, S. C. L. Srivastava, R. Ketzmerick, A. Bäcker, and S. Tomsovic, Entanglement and localization transitions in eigenstates of interacting chaotic systems, Phys. Rev. E **94**, 010205 (2016).

[38] J. Emerson, Y. Weinstein, M. Saraceno, S. Lloyd, and D. G Cory, Pseudo-random unitary operators for quantum information processing, Science **302**, 2098 (2004).

[39] L. Banchi, D. Burgarth, and M. J. Kastoryano, Driven Quantum Dynamics: Will it Blend? Phys. Rev. X **7**, 041015 (2017).

[40] A. Nahum, S. Vijay, and J. Haah, Operator Spreading in Random Unitary Circuits, Phys. Rev. X **8**, 021014 (2018).

[41] S. K. Mishra, A. Lakshminarayan, and V. Subrahmanyam, Protocol using kicked Ising dynamics for generating states with maximal multipartite entanglement, Phys. Rev. A **91**, 022318 (2015).

[42] Y. Y. Atas, E. Bogomolny, O. Giraud, and G. Roux, Distribution of the Ratio of Consecutive Level Spacings in Random Matrix Ensembles, Phys. Rev. Lett. **110**, 084101 (2013).

[43] M. V. Berry, Semiclassical theory of spectral rigidity, Proc. R. Soc. London A **400**, 229 (1985).

[44] M. Lal Mehta, *Random Matrices*, 3rd ed. (Academic Press, New York, 2004).

[45] C. W. von Keyserlingk, T. Rakovszky, F. Pollmann, and S. L. Sondhi, Operator Hydrodynamics, Otocs, and Entanglement Growth in Systems without Conservationlaws, Phys. Rev. X **8**, 021013 (2018).

[46] P. Hosur, X.-L. Qi, D. A. Roberts, and B. Yoshida, Chaos in quantum channels, J. High Energy Phys. 02 (2016) 004.

[47] A. Chan, A. De Luca, and J. T Chalker, Solution of a minimal model for many-body quantum chaos, arXiv:1712.06836.

[48] B. Bertini, P. Kos, and T. Prosen, Exact spectral form factor in a minimal model of many-body quantum chaos, arXiv:1805.00931.

[49] M.-J. Giannoni, A. Voros, and J. Zinn-Justin, *Chaos and Quantum Physics,* Vol. 52, Les Houches Summer School Proceedings Series (North-Holland, Amsterdam, 1991).